Electronic Supplementary Material (ESI) for Journal of Materials Chemistry C.

Electronic Supplementary information

Unfused-ring acceptor enabling ~12% efficiency layer-by-layer organic solar cells

Zhijie Lin,[a] Fuqiang Du,[a] Hongtao Wang[a] Jinru Cao[a] Weihua Tang[a,b]*

[a]*School of Chemical Engineering, Nanjing University of Science and Technology, Nanjing, 210094 P. R. China*

[b]*The Institute of Flexible Electronics (IFE, Future Technologies), Xiamen University, Xiamen, 361005 P. R. China*

**Corresponding authors. E-mail: whtang@xmu.edu.cn*

Table of Content

1. Materials

All reagents and solvents, unless otherwise specified, were purchased from Energy Chemical, Tansoole, J&K, energy chemical or Sigma-Aldrich and were used without further purification. Column chromatography was carried out with 300-400 nm mesh silica. The synthetic routes of ThPF-4F are shown in **Scheme S1**.

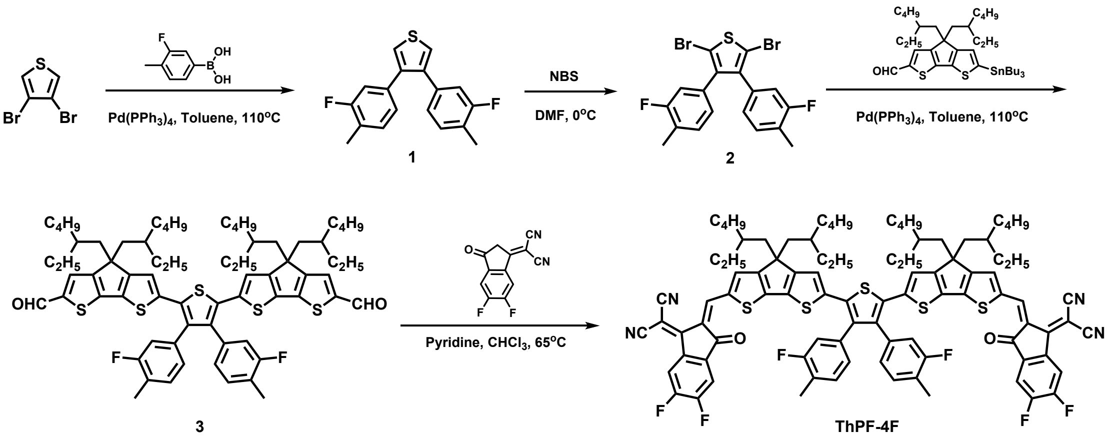

Scheme S1. Synthetic routes of ThPF-4F.

Synthesis of ***compound 1***

A mixture of 3,4-Dibromothiophene (2 g, 8.27 mmol) and 3-Fluoro-4-methylphenylboronic acid (3.82 g, 24.80 mmol, 3 equiv.) in toluene (30 mL) was degassed with N_2 for 20 min before addition of $Pd(PPh_3)_4$ (0.48 g, 0.42 mmol). The reaction mixture was refluxed for 24 h under N_2. The crude compound was purified by column chromatography on silica gel with dichloromethane/petroleum ether (1:5, v/v) to give the title compound **1** as a white solid (2.21 g, 89% yield). ^{1}H NMR (500 MHz, CD_2Cl_2, δ): 7.30 (s, 1H), 7.08 (t, 1H), 6.85 (t, 2H), 2.24 (s, 3H). ^{13}C NMR (125 MHz, CD_2Cl_2, δ): 162.36, 160.42, 140.78, 136.20, 131.61, 124.87, 123.89, 115.78, 14.43.

Synthesis of ***compound 2***

Compound **1** (2 g, 6.66 mmol) was dissolved in a mixture of chloroform and acetic acid (1:1, 20 mL). After cooling in an ice-water bath, the reaction was added with NBS (3.52 g, 19.98 mmol) dropwise in darkness. After reaction overnight, the mixture was diluted with water and extracted with petroleum ether (100 mL). The organic phase was washed with water (2×50 mL) and brine (2×50 mL) before dried over anhydrous Na_2SO_4. The solvents were removed with reduced vacuum. The yellow residue was purified by column chromatography over silica gel (petroleum ether as the eluent) to give the compound **2** as a light yellow oil (2.87 g, 94% yield). ^1H NMR (500 MHz, CD_2Cl_2, δ): 7.09 (t, 1H), 6.77 (t, 2H), 2.23 (s, 3H). ^{13}C NMR (125 MHz, CD_2Cl_2, δ): 162.13, 160.18, 141.37, 134.02, 131.57, 126.11, 117.04, 110.46, 14.56.

Synthesis of ***compound 3***

A mixture of compound **2** (1 g, 2.18 mmol) and 4,4-bis(2-ethylhexyl)-6-(tributylstannyl)-4H-cyclopenta[2,1-b:3,4-b']dithiophene-2-carbaldehyde (4.71 g, 6.55 mmol, 3 equiv.) in toluene (20 mL) was degassed with N_2 for 20 min before addition of $Pd(PPh_3)_4$ (0.13g, 0.11 mmol). The reaction mixture was refluxed overnight under N_2. The crude product was filtered through silica gel, and the filtrate was collected and concentrated. The resulting oil was recrystallized from methanol and used in the next step without further purification.

Synthesis of ***ThPF-4F:***

To the solution of compound **3** (200 mg, 172.7 μmol) in chloroform (20 mL) with pyridine (0.2 mL) was added 2-(5-fluoro-3-oxo-2,3-dihydro-1H-inden-1-ylidene) malononitrile (238.6 mg, 1.04 mmol). After deoxygenated with nitrogen for 20 min, the mixture was refluxed for 3 h. After cooling to room temperature and removal of the solvent under vacuum, the residue was then washed with methanol and hexane. The crude product was purified by silica gel column with petroleum ether/dichloromethane (1:2, v/v) to obtain a dark solid (194.1 mg, 71%). ^1H

NMR (500 MHz, CD_2Cl_2, δ): 8.84 (s, 1H), 8.47 (t, 1H), 7.62 (t, 2H), 7.17 (s, 1H), 7.06 (t, 1H), 6.89 (d, 1H), 6.83 (d , 1H), 2.30 (s, 3H), 1.99 – 1.85 (m, 4H), 0.92 (m , 16H), 0.79 (m, 4H), 0.72 (m , 4H), 0.63 – 0.58 (m, 6H). ^{13}C NMR (125 MHz, CD_2Cl_2, δ): 186.40, 165.51, 162.73, 160.77, 159.91, 158.86, 155.64, 153.54, 144.16, 140.82, 139.43, 138.62, 138.33, 137.02, 136.96, 134.95, 133.47, 132.41, 126.49, 125.97, 121.71, 119.76, 117.38, 117.20, 115.29, 115.15, 115.00, 112.67, 112.53, 68.31, 43.52, 43.41, 35.86, 35.80, 34.56, 34.43, 28.97, 28.83, 27.78, 27.75, 23.25, 23.18, 14.74, 14.33, 14.26, 10.86, 10.71.

2. NMR and mass spectra

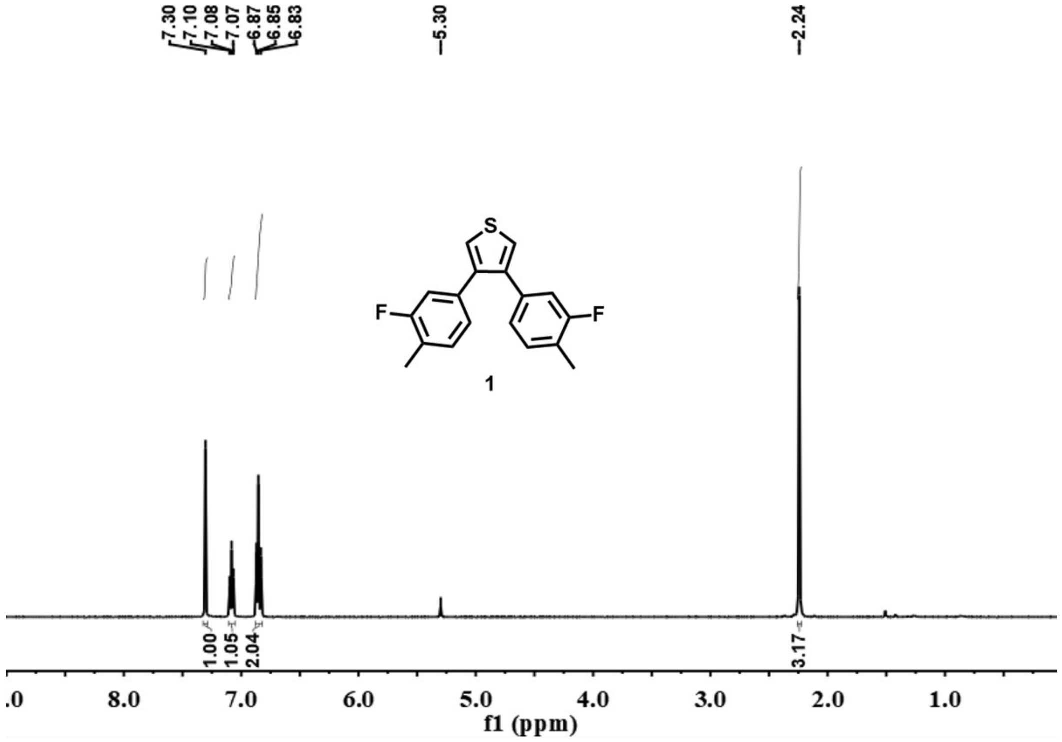

Fig. S1. ^{1}H NMR spectrum of **compound 1**

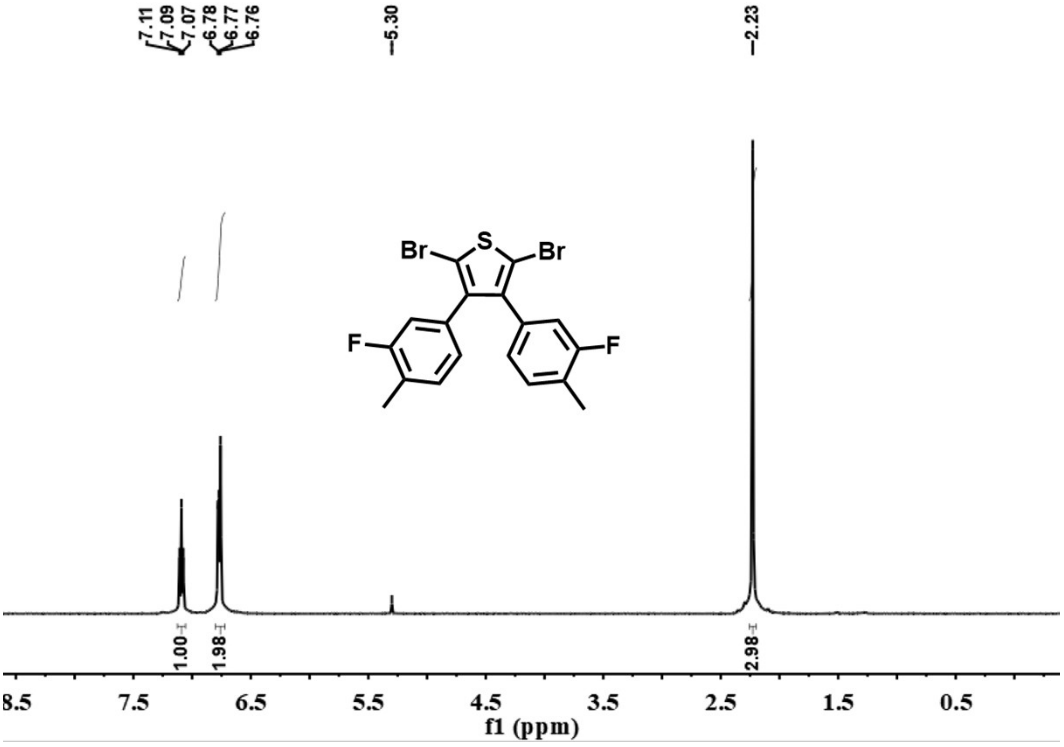

Fig. S2. ^{1}H NMR spectrum of **compound 2**

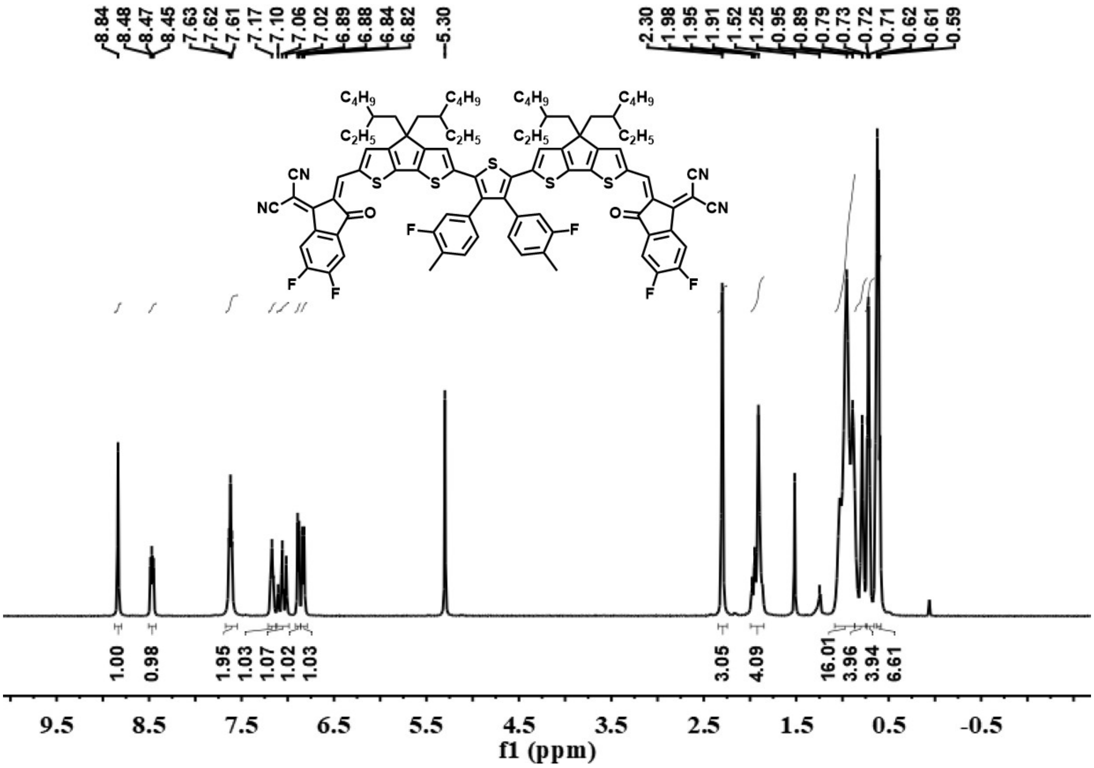

Fig. S3 ^{1}H NMR spectrum of **ThPF-4F**

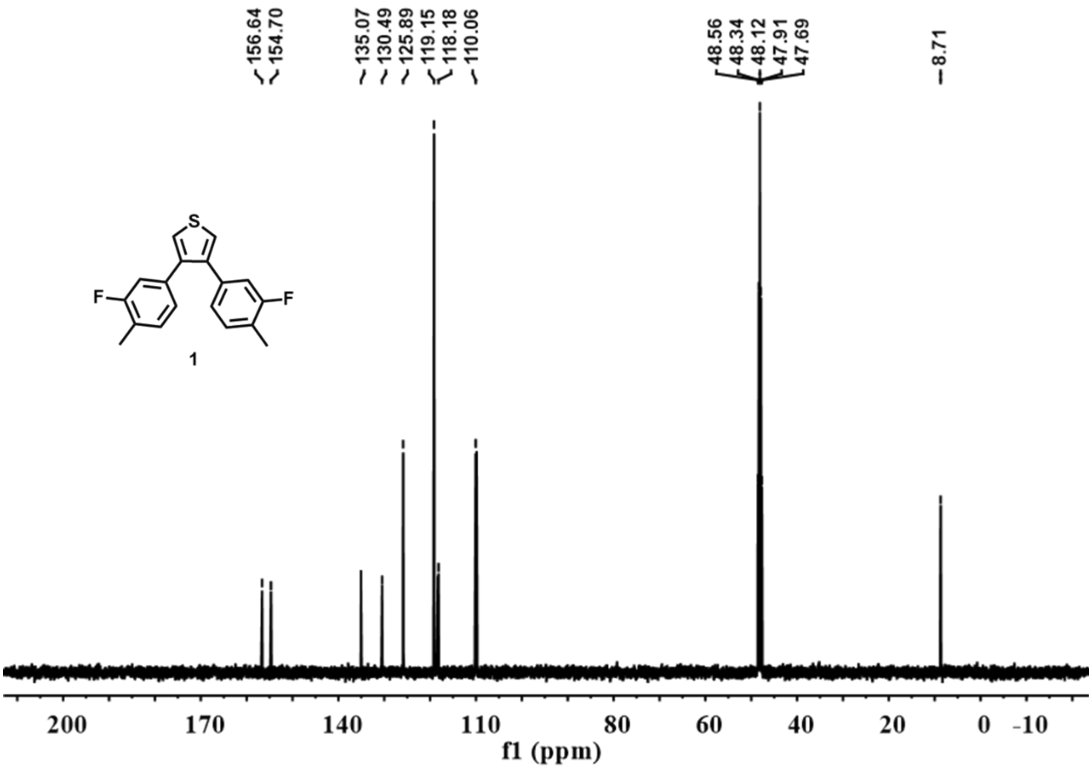

Fig. S4. ^{13}C NMR spectrum of **compound 1**

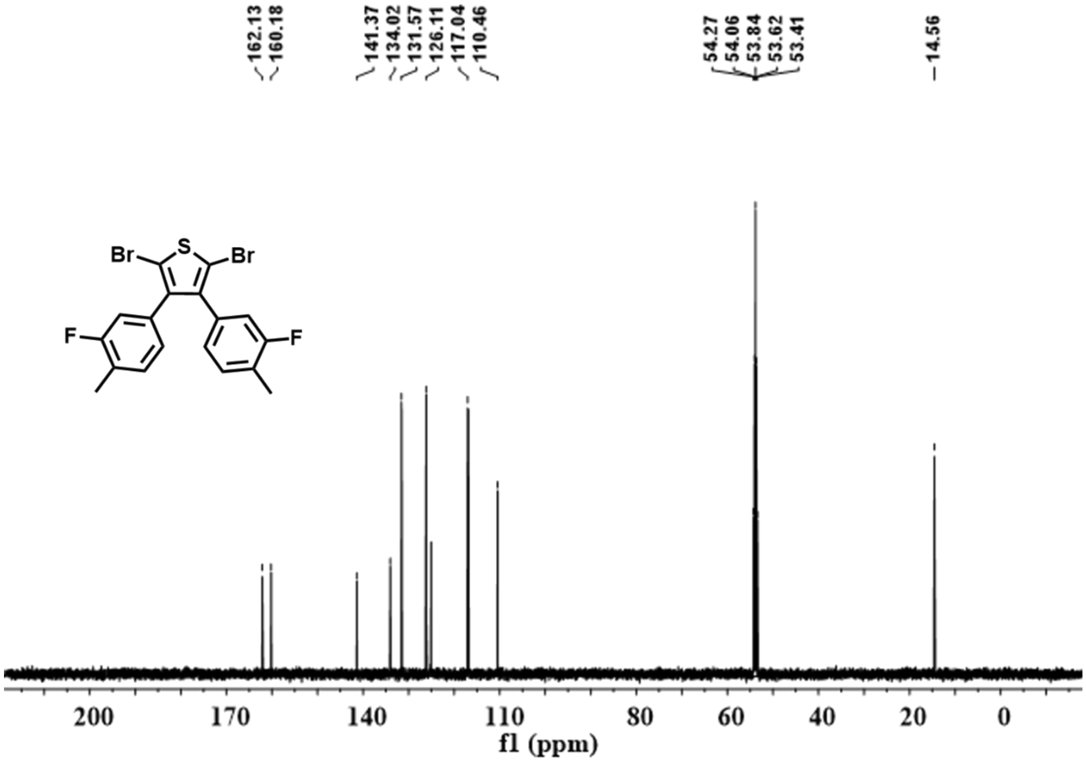

Fig. S5. ^{13}C NMR spectrum of **compound 2**

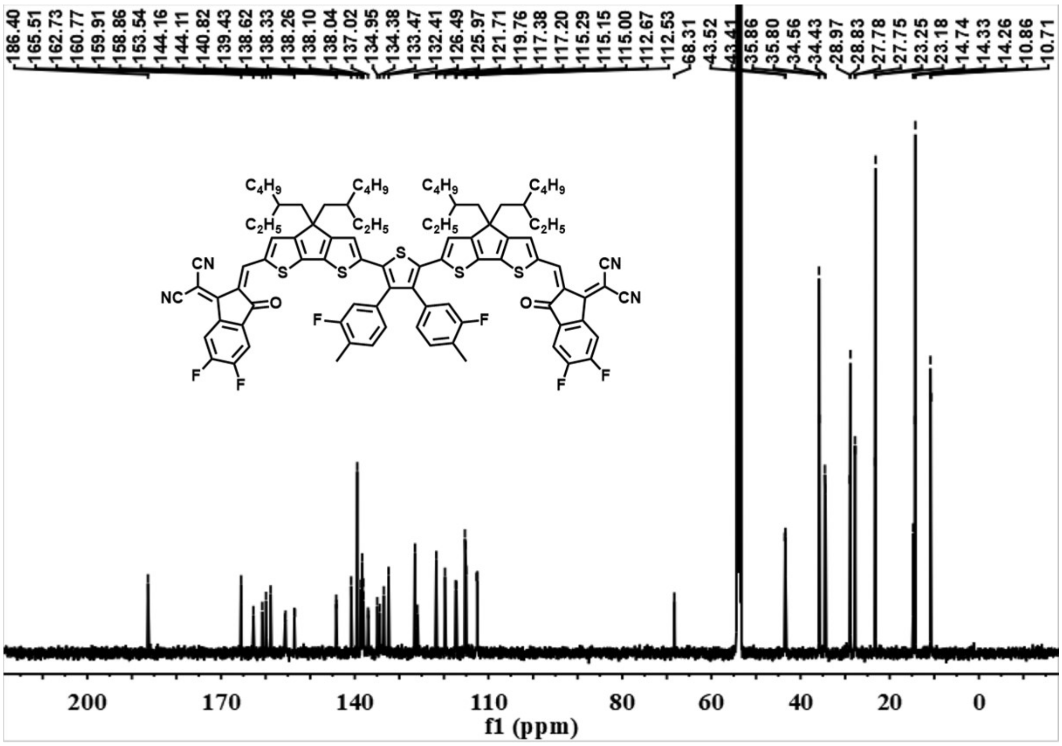

Fig. S6. ^{13}C NMR spectrum of **ThPF-4F**

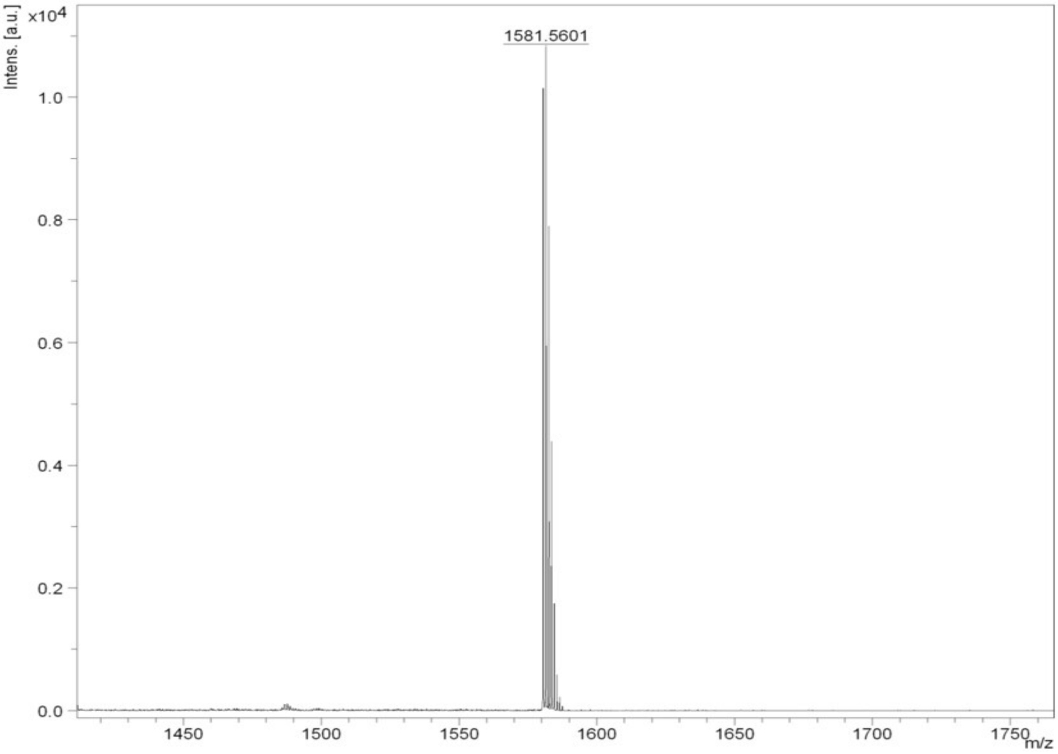

Fig. S7. The MALDI-TOF MS plots of **ThPF-4F**

3. DFT simulation, CV and UV-vis absorption spectra

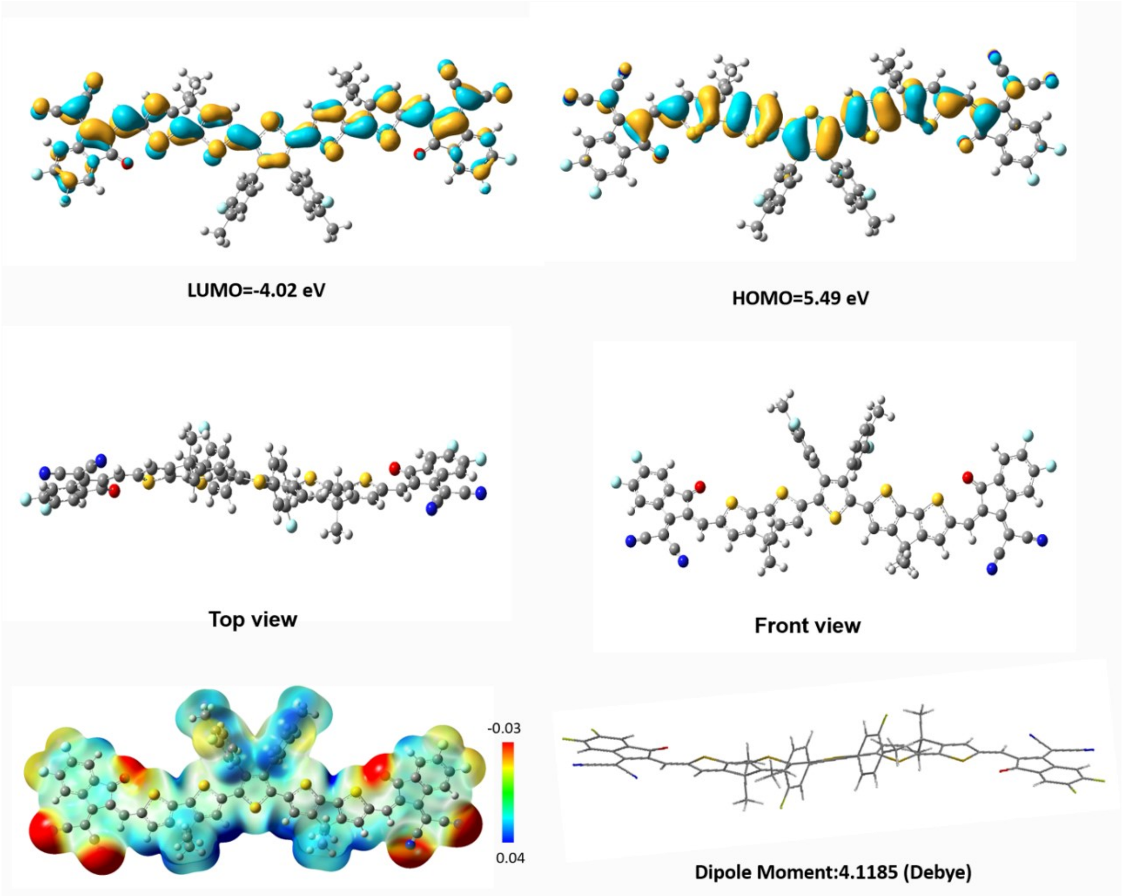

Fig. S8. DFT of ThPF-4F

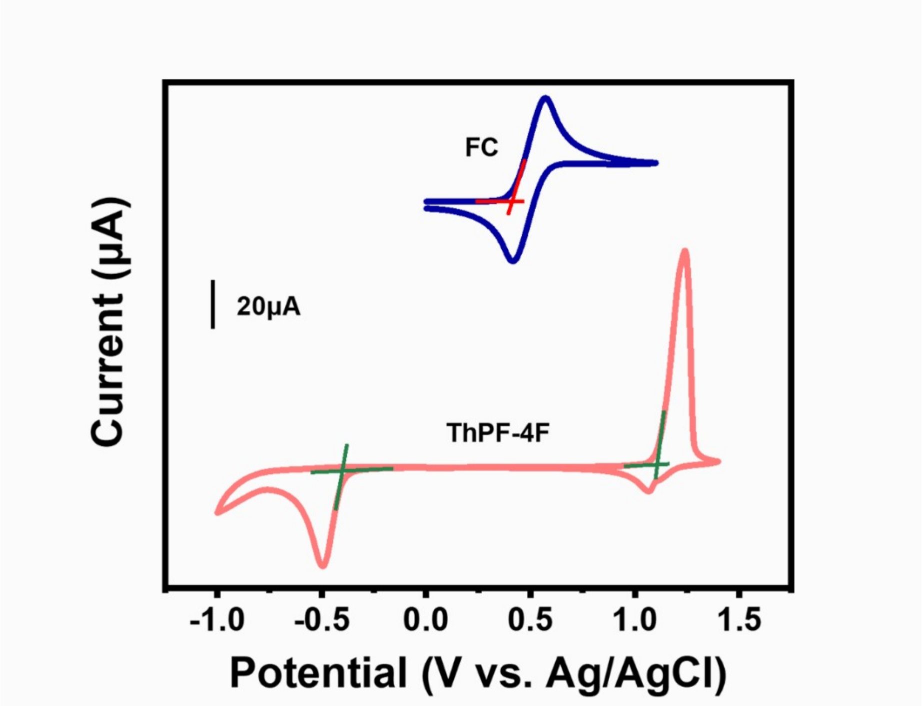

Fig. S9. CV curves of ThPF-4F in chloroform solution

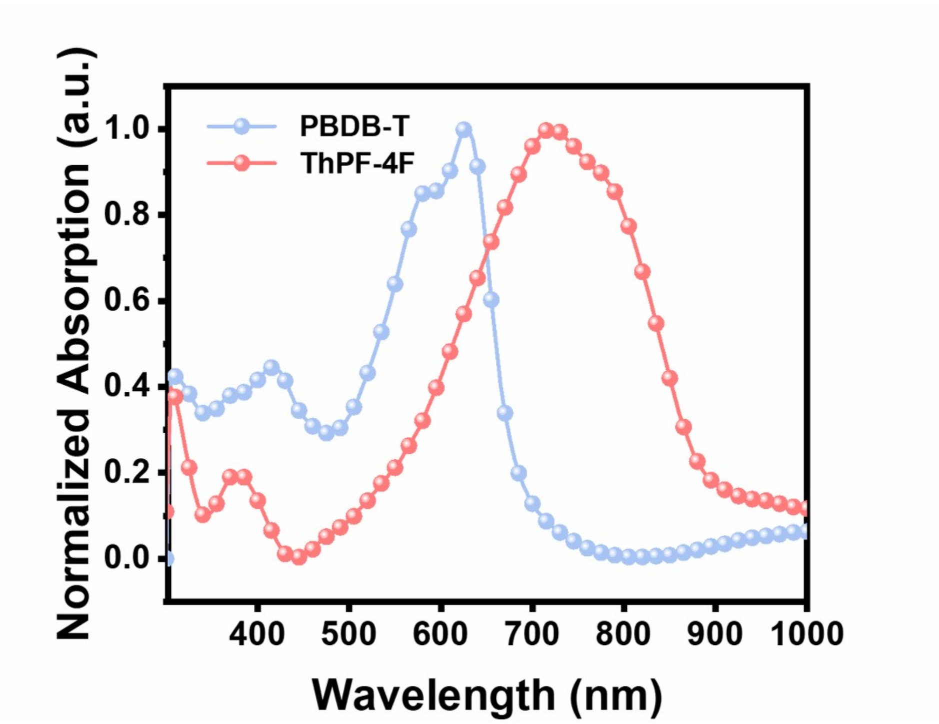

Fig. S10. The UV-vis absorption spectra of the PBDB-T and ThPF-4F

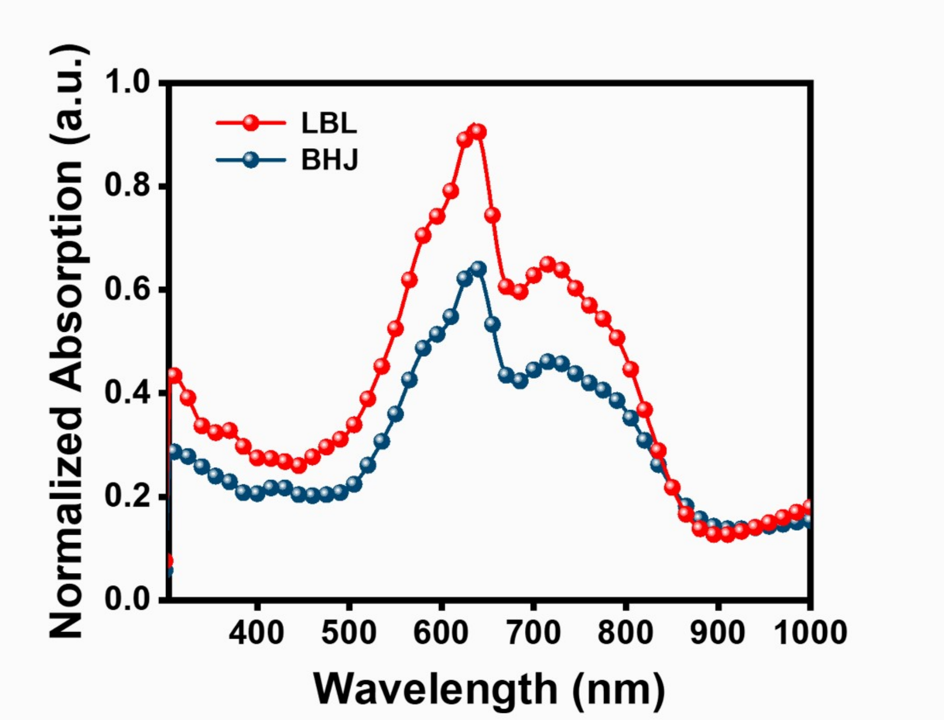

Fig. S11. The UV-vis absorption spectra of LBL device and BHJ blend films

4. Characteristic data of device optimization for BHJ device and LBL device

Table S1. Photovoltaic parameters of BHJ devices with different D/A ratio.

Active layer	D/A	V_{OC} [V] [a]	J_{SC} [mA cm^{-2}] [a]	FF [%][a]	PCE [%][a]
PBDB-T:ThPF-4F	1:0.8	0.84 (0.83±0.01)	18.75 (18.61±0.04)	45.82 (44.72±0.88)	7.22 (6.99±0.16)
	1:1	**0.84** **(0.84±0.01)**	**19.93** **(18.91±0.46)**	**55.98** **(54.61±0.22)**	**9.37** **(9.17±0.14)**
	1:1.2	0.83 (0.83±0.01)	20.65 (20.45±0.10)	49.13 (48.08±0.90)	8.42 (8.21±0.19)

[a] The average values were obtained from 12 devices.

Table S2. Photovoltaic parameters of BHJ devices with different additive.

Active layer	Additive	V_{OC} [V] [a]	J_{SC} [mA cm^{-2}] [a]	FF [%][a]	PCE [%][a]
PBDB-T:ThPF-4F	0.5%DIO	0.80 (0.80±0.01)	16.33 (15.94±0.38)	44.48 (44.06±0.32)	5.81 (5.65±0.15)
	0.5%CN	**0.83** **(0.84±0.01)**	**20.24** **(20.19±0.04)**	**56.03** **(55.64±0.28)**	**9.41** **(9.21±0.16)**

[a] The average values were obtained from over 12 devices

Table S3. Photovoltaic parameters of BHJ devices with different content additive.

Active layer	Additive	V_{OC} [V] [a]	J_{SC} [mA cm^{-2}] [a]	FF [%][a]	PCE [%][a]
PBDB-T:ThPF-4F	0.25%CN	0.84 (0.84±0.01)	19.67 (19.61±0.04)	58.24 (58.05±0.15)	9.63 (9.57±0.04)
	0.5%CN	**0.82** **(0.82±0.01)**	**21.59** **(21.36±0.18)**	**62.20** **(61.87±0.32)**	**11.01** **(10.90±0.07)**
	1%CN	0.83 (0.83±0.01)	19.65 (19.18±0.32)	60.00 (59.03±0.92)	9.79 (9.43±0.26)

[a] The average values were obtained from over 12 devices.

Table S4. Photovoltaic parameters of BHJ devices with different thermal annealing temperature (TAT)

Active layer	TAT [°C]	V_{OC} [V] [a]	J_{SC} [mA cm^{-2}] [a]	FF [%][a]	PCE [%][a]
PBDB-T:ThPF-4F	none	0.83 (0.83±0.01)	20.68 (20.54±0.03)	54.64 (53.81±0.72)	9.38 (9.26±0.11)
	90	0.85 (0.84±0.01)	20.84 (20.68±0.09)	60.70 (59.87±0.14)	10.75 (10.58±0.14)
	100	**0.82** **(0.82±0.01)**	**21.27** **(21.21±0.04)**	**63.65** **(63.41±0.22)**	**11.10** **(11.06±0.04)**
	110	0.82 (0.82±0.01)	21.99 (21.60±0.35)	61.36 (60.59±0.56)	11.06 (10.83±0.21)

[a] The average values were obtained from over 12 devices.

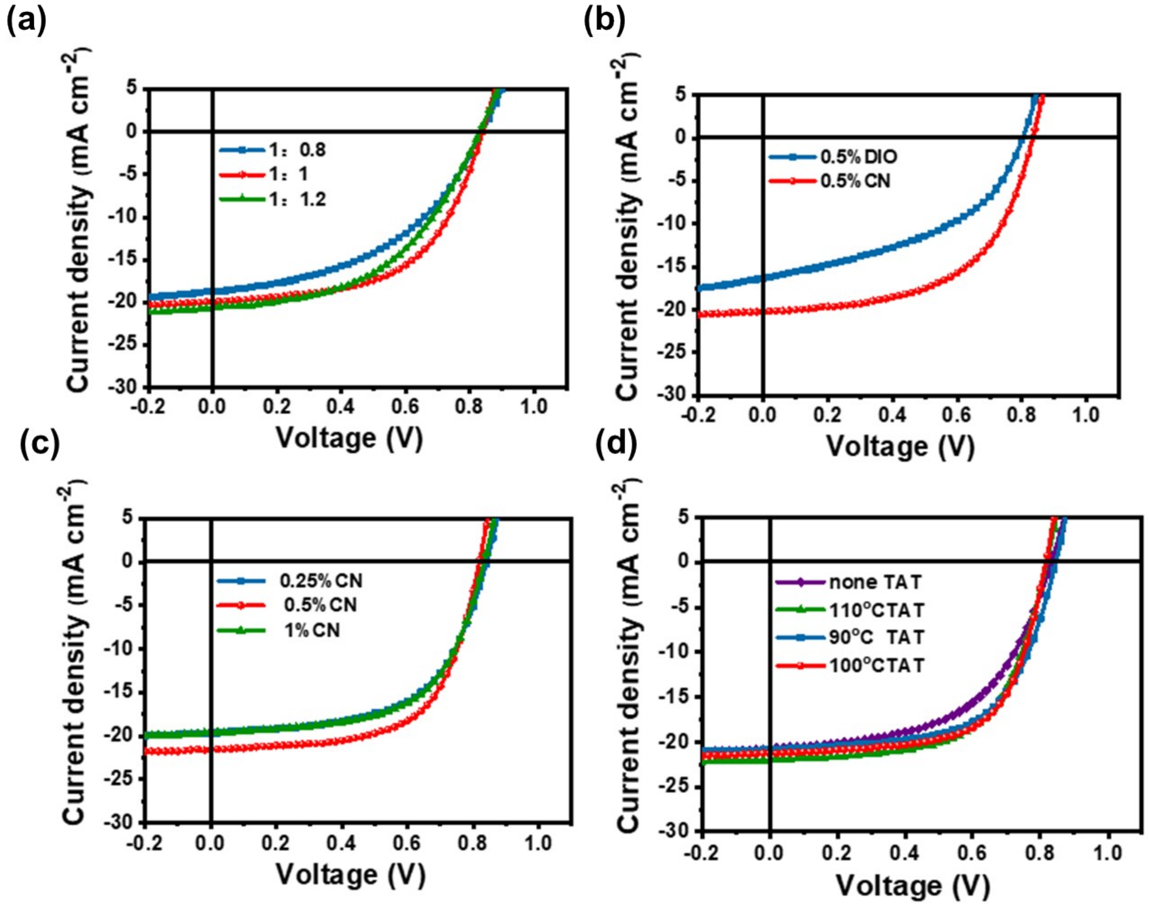

Fig. S12. (a) *J*-*V* curve of BHJ devices with different D/A ratios. (b) *J*-*V* curve of BHJ devices with different additive. (c) *J*-*V* curve of BHJ devices with different content additive. (d) *J*-*V* curve of BHJ devices with different thermal annealing temperature (TAT).

Table S5. The optimized photovoltaic parameters of dual solvent (*o*-DCB:CB) with different *o*-DCB/CB ratio.

Donor	Acceptor	V_{OC} [V] [a]	J_{SC} [mA cm^{-2}] [a]	FF [%][a]	PCE [%][a]
o-DCB	CB	0.82 (0.81±0.01)	14.07 (13.49±0.57)	60.39 (60.02±0.19)	6.97 (6.42±0.45)
o-DCB:CB=7:3	CB	0.83 (0.83±0.01)	21.18 (21.04±0.12)	55.73 (54.84±0.78)	9.80 (9.58±0.17)
***o*-DCB:CB=4:1**	**CB**	**0.82** **(0.82±0.01)**	**21.37** **(21.22±0.05)**	**58.59** **(57.60±0.96)**	**10.27** **(9.92±0.28)**
o-DCB:CB=9:1	CB	0.81 (0.81±0.01)	22.58 (22.53±0.02)	52.82 (52.06±0.72)	9.66 (9.55±0.10)
CB	CB	0.72 (0.71±0.01)	12.83 (12.49±0.31)	52.44 (51.65±0.59)	4.84 (4.63±0.16)

[a] The average values were obtained from over 12 devices.

Table S6. The optimized photovoltaic parameters of LBL OSCs with different concentration.

Donor [mg/mL]	Acceptor [mg/mL]	V_{OC} [V] [a]	J_{SC} [mA cm^{-2}] [a]	FF [%][a]	PCE [%][a]
10	10	0.83 (0.83±0.01)	16.48 (16.21±0.23)	64.95 (64.50±0.37)	8.88 (8.70±0.15)
13.5	13.5	**0.82** **(0.82±0.01)**	**21.68** **(21.61±0.03)**	**56.95** **(56.57±0.28)**	**10.13** **(10.03±0.06)**
15	15	0.83 (0.83±0.01)	22.35 (21.96±0.36)	51.17 (50.27±0.56)	9.49 (9.10±0.36)

[a] The average values were obtained from over 12 devices.

Table S7. The optimized photovoltaic parameters of LBL OSCs with different content additive.

Active layer	Additive	V_{OC} [V] [a]	J_{SC} [mA cm^{-2}] [a]	FF [%][a]	PCE [%][a]
PBDB-T/ ThPF-4F	0.25%CN	0.83 (0.83±0.01)	21.32 (21.05±0.26)	56.50 (56.12±0.37)	10.00 (9.99±0.01)
	0.5%CN	**0.82** **(0.83±0.01)**	**21.66** **(21.10±0.33)**	**62.56** **(62.42±0.08)**	**11.11** **(10.94±0.14)**
	1%CN	0.82 (0.82±0.01)	20.73 (20.38±0.23)	58.33 (57.36±0.75)	9.92 (9.79±0.12)

[a] The average values were obtained from over 12 devices.

Table S8. The optimized photovoltaic parameters of LBL OSCs with different spin coating speed (RPM).

Donor [RPM]	Acceptor [RPM]	V_{OC} [V] [a]	J_{SC} [mA cm^{-2}] [a]	FF [%] [a]	PCE [%] [a]
2000	2500	0.83 (0.83±0.01)	21.40 (21.08±0.16)	62.53 (62.11±0.20)	11.11 (10.97±0.13)
2500	2500	0.82 (0.82±0.01)	21.44 (21.31±0.13)	64.31 (63.95±0.29)	11.31 (11.06±0.23)
2500	**2750**	**0.81** **(0.82±0.01)**	**22.20** **(22.13±0.01)**	**65.79** **(63.96±0.54)**	**11.83** **(11.36±0.29)**
2750	2500	0.82 (0.82±0.01)	20.92 (20.62±0.21)	63.43 (63.05±0.31)	10.88 (10.76±0.02)
2500	3000	0.83 (0.82±0.01)	21.37 (21.32±0.04)	63.63 (63.24±0.31)	11.29 (11.17±0.09)

[a] The average values were obtained from over 12 devices.

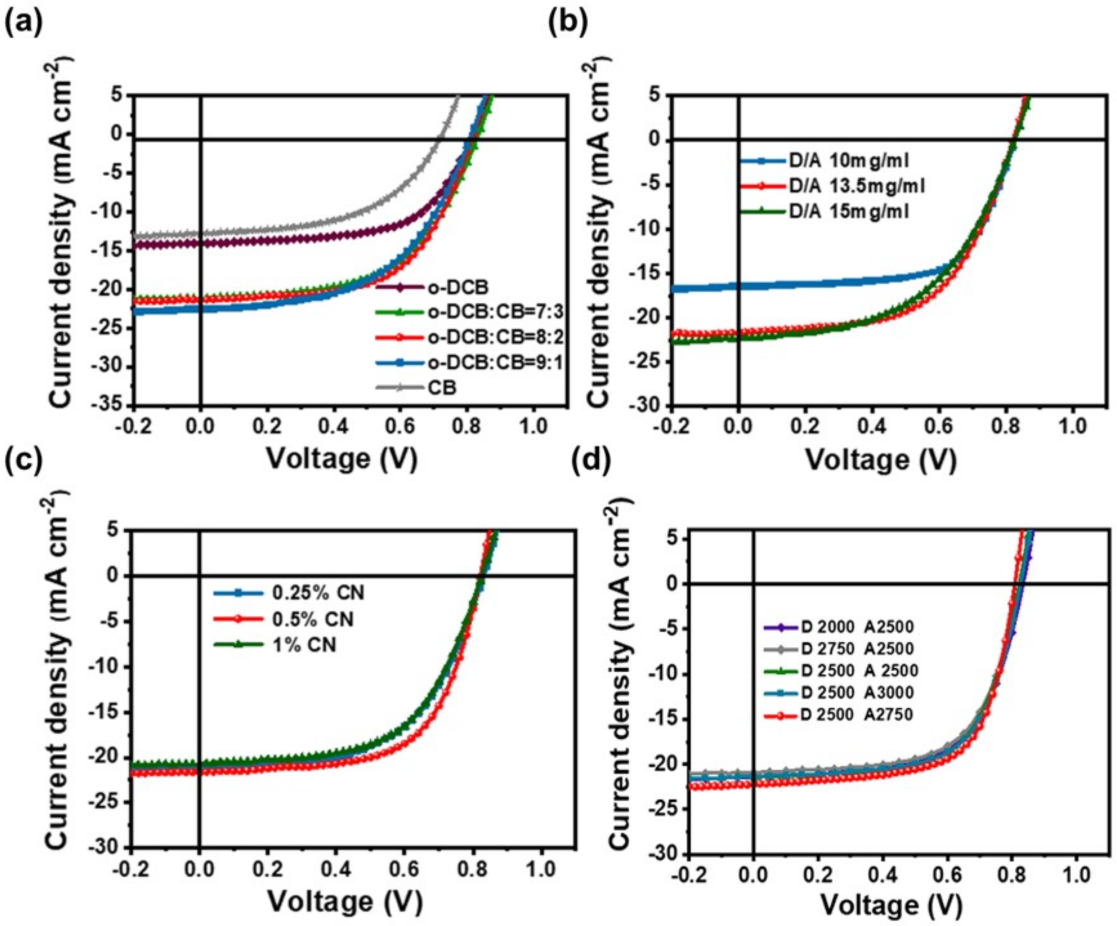

Fig. S13. (a) *J*-*V* curves of o-DCB:CB with different ratio value. (b) *J*-*V* curves of D/A with different concentration. (c) *J*-*V* curves of additive with different ratio value. (d) *J*-*V* curves of D/A with different spin coating speed.

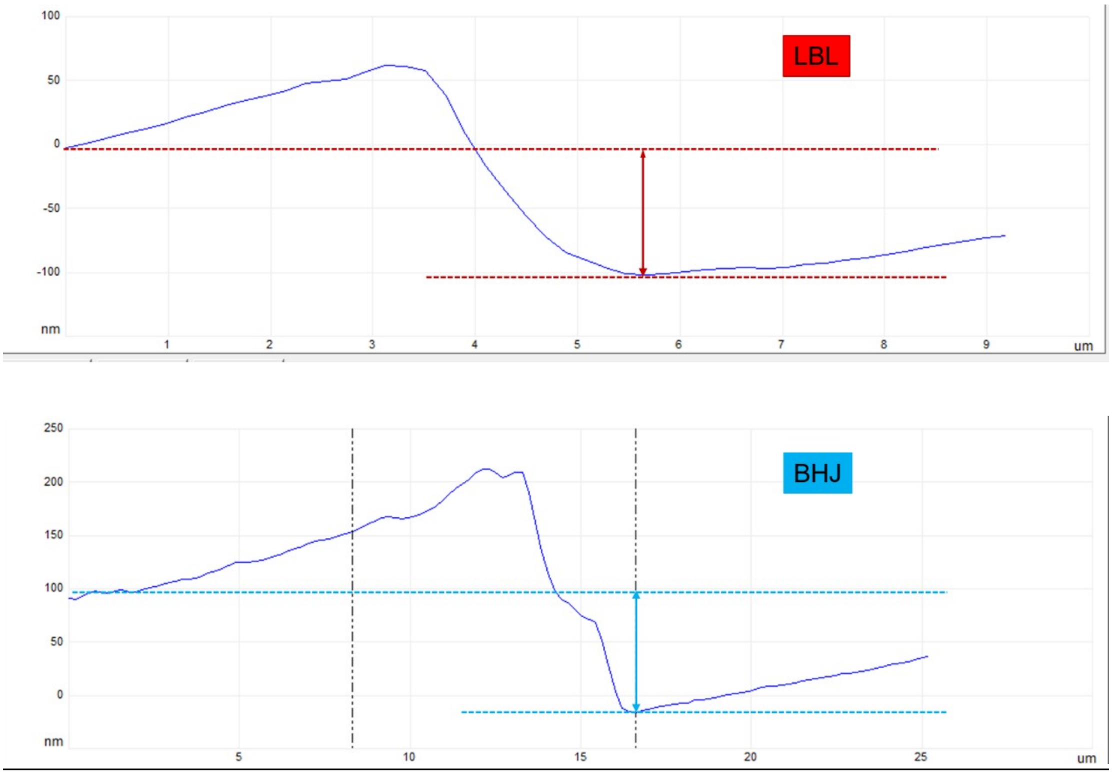

Fig. S14. Active layer thickness of LBL and BHJ devices measured by AFM.

5. Mobility data

Nano ZnO electron transport layer in the manuscript as follows. Zinc acetate dihydrate ($Zn(CH_3COO)_2 \cdot 2H_2O$, Aldrich, 99.9%, 0.5 g) was added to 2-methoxyethanol ($CH_3OCH_2CH_2OH$, Aldrich, 99.8%, 5 mL) and ethanolamine ($NH_2CH_2CH_2OH$, Aldrich, 99.5%, 140 uL) as the precursor solution. Mix and stir in the glove box for more than 5 hours. During spin coating, filter out the impurities with a 0.22 μm polytetrafluoroethylene (PTFE) filter head. Spin-coating speed of 4000 rpm and spin coating time of 30 s. Complete the annealing operation on the heating plate, the annealing temperature is 85 °C and the annealing time is 10 mins. After the annealing is completed, then transferred out of the glove box. By completing the oxidation step in atmospheric atmosphere, i.e., complete the second anneal on the heating plate (180 °C for 30 mins), 30 nm sol-gel derived ZnO film is prepared.

Table S9. Hole and electron mobilities of PBDB-T:ThPF-4F and PBDB-T/ThPF-4F blends.

Device	μ_h [cm^2 V^{-1} s^{-1}]	μ_e [cm^2 V^{-1} s^{-1}]	μ_h/μ_e
LBL OSCs	$3.11*10^{-5}$	$6.81*10^{-6}$	4.57
BHJ OSCs	$2.67*10^{-5}$	$4.97*10^{-6}$	5.37

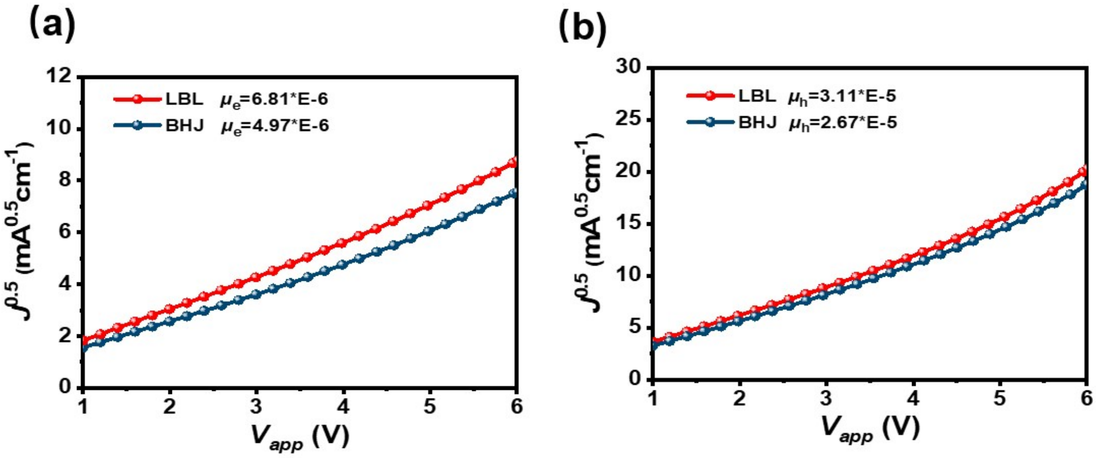

Fig. S15. $J^{0.5}$-V characteristics were acquired from (a) electron -only and (b) hole-only devices based on BHJ OSCs and LBL OSCs.

6. Optical exciton generation rate

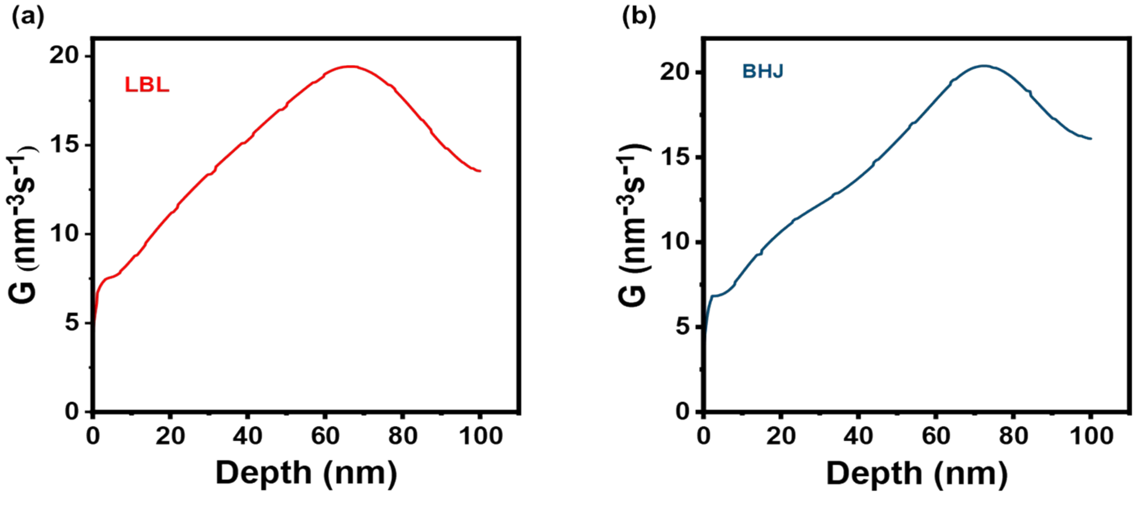

Fig. S16. Optical exciton generation rate (G) curves of LBL(a) and BHJ (b) devices.

7. Contact Angle Measurement

$$\gamma_{water}\left(1+cos\theta_{water}\right)=\frac{4\gamma_{water}^{d}\gamma^{d}}{\gamma_{water}^{d}+\gamma^{d}}+\frac{4\gamma_{water}^{p}\gamma^{p}}{\gamma_{water}^{p}+\gamma^{p}} \qquad (1)$$

$$\gamma_{diiodomethane}\left(1+cos\theta_{diiodomethane}\right)=\frac{4\gamma_{diiodomethane}^{d}\gamma^{d}}{\gamma_{diiodomethane}^{d}+\gamma^{d}}+\frac{4\gamma_{diiodomethane}^{p}\gamma^{p}}{\gamma_{diiodomethane}^{p}+\gamma^{p}} \qquad (2)$$

$$\gamma=\gamma^{d}+\gamma^{p} \qquad (3)$$

where γ^{d} and γ^{p} are the dispersion and polar components of γ; γ_i^{d} and γ_i^{p} are the dispersion and polar components of γ_i; and θ is the droplet contact angle (water or diiodomethane) on neat films.[1]

Table S10. Contact angle measurement of PBDB-T, ThPF-4F neat films and PBDB-T:ThPF-4F, PBDB-T/ThPF-4F blend films.

Pure film	θ_{water} (deg)	$\theta_{\mathrm{diiodomethane}}$ (deg)	γ (mN m^{-1})
PBDB-T	103.07°	54.78°	33.09
ThPF-4F	102.85°	44.62°	39.01

Blend film	θ_{water} (deg)	$\theta_{\mathrm{diiodomethane}}$ (deg)	γ (mN m^{-1})
PBDB-T:ThPF-4F (BHJ)	92.68°	58.78°	33.46
PBDB-T/ThPF-4F (LBL)	104.74°	56.10°	32.68

Reference

1. Jiang, G. Zhang, G. Yang, J. Zhang, Z. Li, T. Ma, H. Hu, W. Ma, H. Ade and H. Yan, *Adv. Energy Mater.*,

2018, **8**, 1701370.